SUPPORTING INFORMATION

On chip Steady liquid-gas phase separation for flexible generation of dissolved gas concentration gradient

Bi-Yi Xu, Shan-Wen Hu, Xiao-Na Yan, Xing-Hua Xia, Jing-Juan Xu*, Hong-Yuan Chen

State Key Laboratory of Analytical Chemistry for Life Science, School of Chemistry and Chemical Engineering, Nanjing University, Nanjing 210093, China.

Email: xujj@nju.edu.cn,

Table S1. Summary for characteristics of typical gas dissolving interface for microfluidic chips

No.	Liquid-gas interface type	Gas dissolving type and rate	Gradient generation & stability	Application	Ref.
1	Gas bubbling	Air Rate not mentioned	Generate convective flux, no stable gradient available	Room NH_3 monitoring	6
2	PDMS membrane (15 μm thick)	Air 50~200 ml/min/m^2	Not mentioned	Artificial lung	4
3	PDMS membrane (50 μm thick)	O_2 Rate not mentioned	Not mentioned	Photosensitized organic oxygenation reaction	7
4	PDMS membrane (100 μm thick)	O_2 <20s for O_2 to perfuse through the membrane	Oxygen gradient generated	Cell culture under different O_2 concentrations	2
5	PDMS membrane (~200 μm thick)	CO_2 Total acidification after 9.5 min	Not mentioned		8
6	3D interconnected micro-porous PDMS (~200 μm thick)	CO_2 Total acidification within 90s	Observable gradient	Potential application for cell culture	
7	SMA array bridge	CO_2 Total acidification within 90s	Stable gradient with certain degree of flexibility	$CaCO_3$ deposition reaction	Present work

Details for Physical modeling of DgCG

For DgCG modeling, Comsol multiphysics 3.5 is applied. The gradient system can be physically described by combining the steady state ***incompressible Navier-Stocks equation***:

$$\rho((u\cdot\nabla)u) = -\nabla\cdot p + \eta(\nabla^2 u) \qquad (1)$$

$$\nabla \cdot u = 0 \qquad (2)$$

and the ***convection and diffusion equation***:

$$D\nabla^2 c = u \cdot \nabla c \qquad (3)$$

ρ, u, p and η are the density, flow velocity field, pressure and the viscosity of the liquid. D and c are diffusion coefficient and dissolved gas concentration. The two equations are coupled together by sharing the 2D flow velocity field u. The detailed parameters and settings for the models share the following values.

Table S2. NS-equation boundary condition for **Model S1** and **Model S2**

Boundary	Condition	Value
Inlet	Velocity	U_0
Outlet	Pressure	0
Gas-liquid interface	No slip	-
Wall	No slip	-

Table S3. Convection and diffusion boundary condition for **Model S1** and **Model S2**

Boundary	Condition	Value
Inlet	Concentration	0 mol/m^3
Outlet	Convective flux	-
Gas-liquid interface	Concentration	1 mol/m^3
Wall	Insulation	-

Table S4. Physical data for subdomain settings for **Model S1** and **Model S2**

Physical quantity	Value
Diffusion coefficient for CO_2 (isotropic) D	1.77e-9m^2/s
Initial concentration for CO_2 c_0	0 mol/m^3
x-velocity	u (the x direction component of u)
y-velocity	v (the y direction component of u)
Liquid density ρ	1 kg/m^3
Liquid Dynamic viscosity η	1 Pa*s
Liquid Volume force	0 N/ m^3

Table S5. Geometrical settings for **Model S1**

Geometrical parameters	Value
SMA single channel width	10, 20, 30, 40, 50 µm
SMA interspaces	100, 150, 200, 300, 500 µm
SMA inlet flow velocity	0.1, 0.2, 0.5, 1.0, 2.0 µL/min

The two dimensional simulations are performed in a triangular grid consisting of 23430 cells for model 1 and 54769 cells for model 2. The densities of the triangular grid are chosen to best adapt the geometry of the models for high quality results.

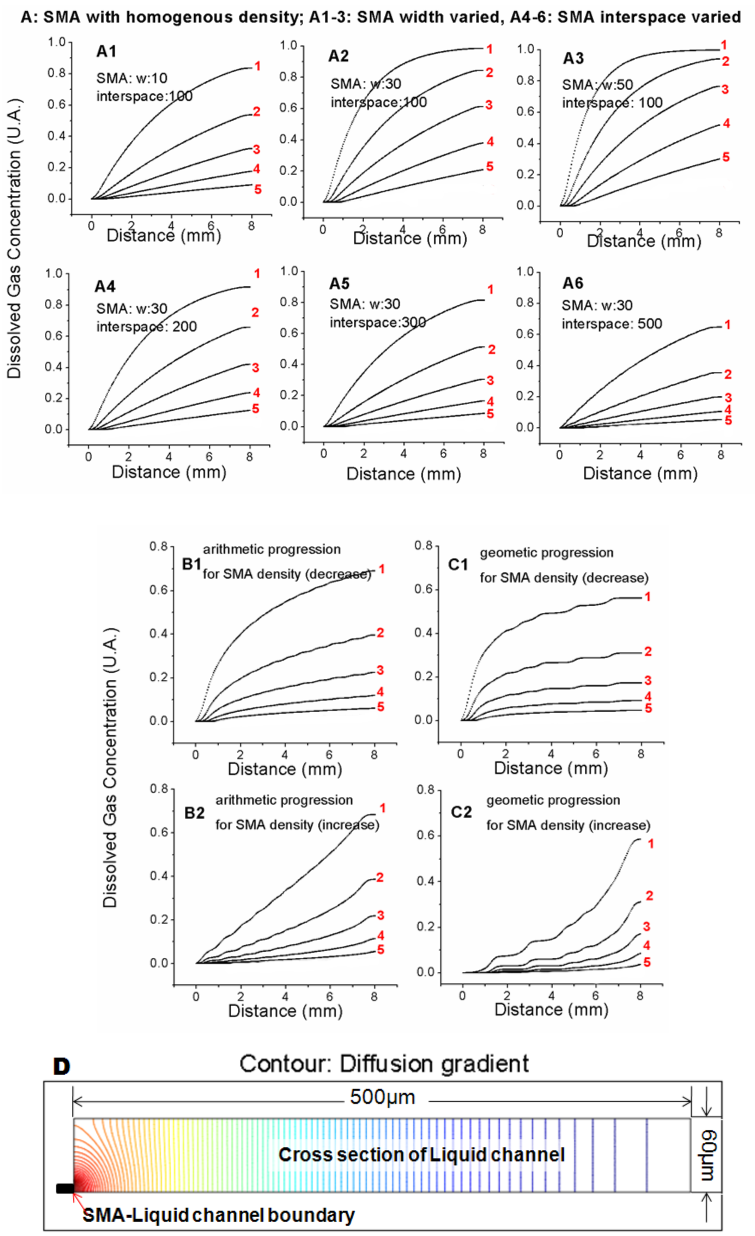

Figure S1. Modelled results for concentration profiles along the centreline of the liquid channel with different geometries and distribution of the SMA. 1 to 5 corresponds to inlet velocity from 0.1, 0.2, 0.4, 0.8 to 1.6 µL/min. A1-6. Homogenous SMA distribution. A1-3. the small channels are equally interspaced of 100 µm, but of different channel width (10, 30, 50 µm). A4-6. the small channels are of different interspaces (200, 300, 500 µm) but same channel width of 30 µm. B1-2. Arithmetic progression for SMA distribution. C1-2. Geometric progression for SMA distribution. D. distribution of the diffusion gradient

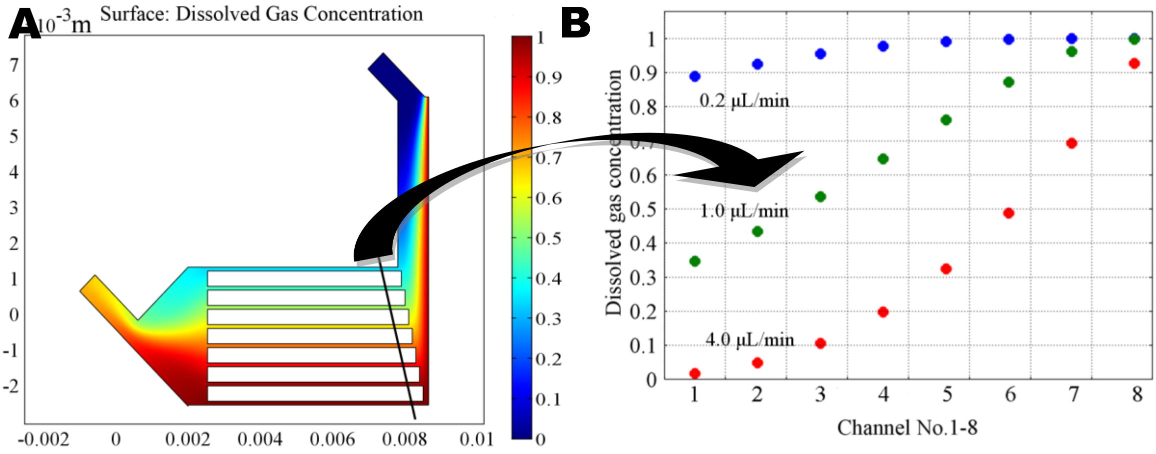

Figure S2. The CO_2 concentration distribution in model S2. A. the CO_2 concentration distribution under inlet flow velocity of 1.0 μL/min, B. the dissolved CO_2 concentration in the 8 channels under inlet flow velocity of 0.2, 1.0, 4.0 μL/min. The local concentration is normalized based on the scale that the saturation concentration is 1.

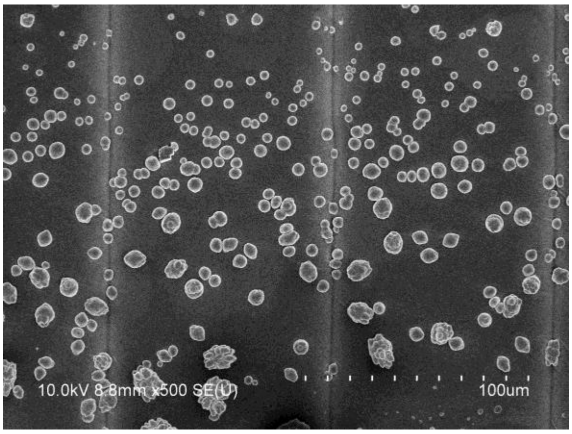

Figure S3. Birds view for the generated $CaCO_3$ in the channel near the liquid-gas interface in the major channel (region of dotted red frame in figure 4B). The top of the image is near the liquid-gas interface.

Transforming the color information to CO_2 content

To transform the color information to the related content of the dissolved carbon dioxide, we did the following experiment.

First, the colors of solutions under different pH are recorded in standard condition.

Second, to link the pH to the carbon dioxide concentration, calculations are carried out to estimate the amount of carbon dioxide needed to transform the bromythel blue solution (containing 10 mM NaOH) to a certain pH. The calculations are based on the principle for acid-base equilibrium.

$H_2CO_3 \rightleftharpoons H^+ + HCO_3^-$ (1), with K_{a1}, suppose x molar H^+ has been generated.

$HCO_3^- \rightleftharpoons H^+ + CO_3^{2-}$ (2), with K_{a2} suppose y molar H^+ has been generated.

$H_2O \rightleftharpoons H^+ + OH^-$ (3), with K_w suppose z molar H^+ has been generated.

	H_2CO_3	HCO_3^-	CO_3^{2-}	OH^-	H^+
Start	a	b	c	d	0
Equilibrium	a-x	b+x-y	c+y	d+z	x+y+z

Based on the above relationship, it can be deduced:

$$\left.\begin{aligned} K_{a1} &= \frac{(b+x-y)*(x+y+z)}{(a-x)} \\ K_{a2} &= \frac{(c+y)*(x+y+z)}{(b+x-y)} \\ K_w &= (d+z)*(x+y+z) \end{aligned}\right\} \Rightarrow \left\{\begin{aligned} K_{a1} &= \frac{(b+x-y)*K_w}{(a-x)*(d+z)} (4) \\ K_{a2} &= \frac{(c+y)*K_w}{(b+x-y)*(d+z)} (5) \\ K_w &= (d+z)*(x+y+z) (6) \end{aligned}\right.$$

Where K_{a1}=4.3*10^{-7}, K_{a2}=5.6*10^{-11}, K_w=10^{-14}

The equations are solved for the content of H^+, using following values corresponding to a, b, c and d as is shown in the following table. The content of H^+ is then transformed to pH. To solve the equations, the software Mathematica 5 is applied. Curve fittings are applied for the relationship between the CO_2%~pH with the help of Matlab 7.0 curve fitting tools. The original solution is pH=12, and the CO_2 saturated solution is pH=6.1.

Table S6. Relationship between pH and the content of carbon dioxide.

NaOH (d)	Na_2CO_3 (c)	$NaHCO_3$ (b)	H_2CO_3 (a)	CO_2 content (Mol)	pH (calculated)	CO_2 content %
0.01				0	12.0000	0
0.008	0.001			0.001	11.9043	3.624633
0.006	0.002			0.002	11.7823	7.249266
0.004	0.003			0.003	11.6154	10.8739
0.002	0.004			0.004	11.3597	14.49853
0	0.005	0		0.005	10.9344	18.12317
	0.004	0.002		0.006	10.4616	21.7478
	0.003	0.004		0.007	10.0954	25.37243
	0.002	0.006		0.008	9.75881	28.99706
	0.001	0.008		0.009	9.34252	32.6217
	0.0005	0.009		0.0095	9.00695	34.43401
	0.0002	0.0096		0.0098	8.66063	35.5214
	0	0.01	0	0.01	8.30525	36.24633

Electronic Supplementary Material (ESI) for Lab on a Chip

	0.01	0.0001	0.0101	8.11961	36.60879
	0.01	0.0002	0.0102	7.96134	36.97126
	0.01	0.0005	0.0105	7.64423	38.05865
	0.01	0.001	0.011	7.35981	39.87096
	0.01	0.002	0.012	7.06353	43.4956
	0.01	0.005	0.015	6.66713	54.3695
	0.01	0.01	0.02	6.36640	72.49266
	0.01	0.015	0.025	6.19030	90.61583
	0.01	0.02	0.03	6.06549	>100

Last, the location with the same color as the recorded with known pH are transformed to the content of CO_2 as are imaged in Fig. 4 A3 in the text.